Title: A liquid chromatography high-resolution mass spectrometry *in vitro* assay to assess metabolism at the injection site of subcutaneously administered therapeutic peptides

Authors: Simone Esposito, Maria Lucia de Leonibus, Raffaele Ingenito, Elisabetta Bianchi, Laura Orsatti, Edith Monteagudo

PII: S0731-7085(18)31245-7
DOI: https://doi.org/10.1016/j.jpba.2018.07.009
Reference: PBA 12080

To appear in: *Journal of Pharmaceutical and Biomedical Analysis*

Received date: 31-5-2018
Revised date: 6-7-2018
Accepted date: 9-7-2018

Please cite this article as: Esposito S, de Leonibus ML, Ingenito R, Bianchi E, Orsatti L, Monteagudo E, A liquid chromatography high-resolution mass spectrometry *in vitro* assay to assess metabolism at the injection site of subcutaneously administered therapeutic peptides, *Journal of Pharmaceutical and Biomedical Analysis* (2018), https://doi.org/10.1016/j.jpba.2018.07.009

A liquid chromatography high-resolution mass spectrometry *in vitro* assay to assess metabolism at the injection site of subcutaneously administered therapeutic peptides

Simone Esposito[a], Maria Lucia de Leonibus[a], Raffaele Ingenito[b], Elisabetta Bianchi[b], Laura Orsatti[a], Edith Monteagudo[a,*]

[a]DMPK and [b]Peptide Therapeutics, IRBM Science Park, Via Pontina km 30,600, 00071 Pomezia (Roma), Italy

*: Corresponding author – Email: monteagudo@irbm.it

Graphical abstract

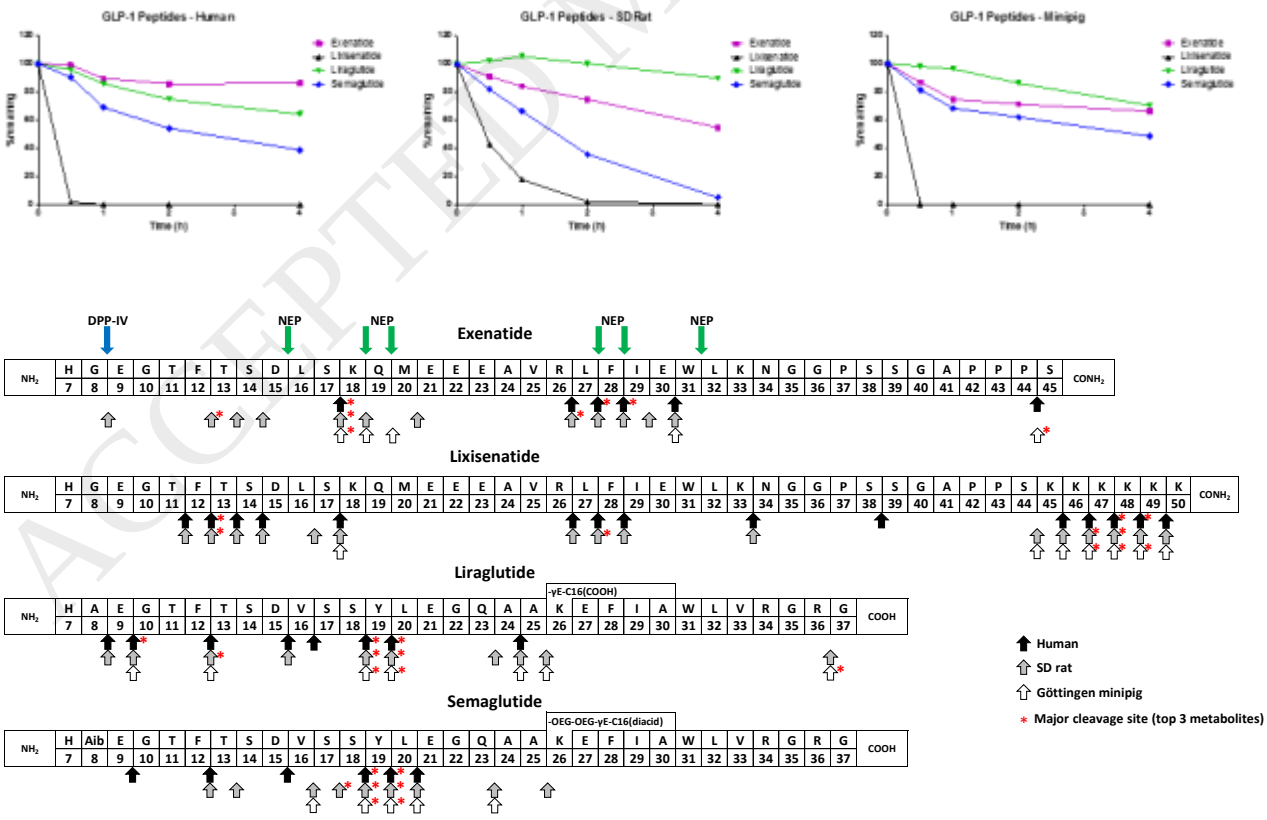

Highlights

- An *in vitro* LC-HRMS assay to predict peptide subcutaneous metabolism
- In vitro half-life is calculated and metabolites are identified in a single assay
- Good *in vitro/in vivo* correlation was obtained for human and preclinical species
- The assay can be used to improve peptide subcutaneous bioavailability

Abstract

Subcutaneous (SC) injection is the most common administration route for peptide therapeutics. Catabolism at the injection site can be a specific and major degradation pathway for many SC administered peptides. In some cases, it can significantly affect pharmacokinetics, particularly bioavailability, and have detrimental effects on the efficacy of the drug.

This work describes a liquid chromatography-high resolution mass spectrometry based in vitro assay to assess peptide metabolism in the SC tissue (SCiMetPep assay). The SCiMetPep assay was developed using human, Sprague-Dawley rat and Göttingen minipig SC tissue homogenate supernatant, and allows for both determination of degradation rate (half-life) of the parent peptide and identification of metabolites generated from enzymatic proteolysis.

The assay was developed and validated using known peptides including human insulin and four GLP-1 analogues (lixisenatide, exenatide, liraglutide and semaglutide). Different experimental parameters were evaluated in order to optimize the homogenization process of the SC tissue and the peptide incubation conditions. *In vitro* metabolism of these peptides was in good agreement with *in vivo* data reported in the literature. Finally, when SCiMetPep assay was applied on a series of structurally related peptides, a fairly good correlation was found between SC metabolic stability and bioavailability, suggesting that catabolism at the injection site can have a major role in the absorption, distribution, metabolism, and excretion (ADME) of peptide therapeutics. The SCiMetPep showed the ability to identify analogs with improved SC metabolic stability and hence higher bioavailability. The assay can be used in the early phases of drug discovery to identify peptide metabolic soft spots at the injection site and guide the peptide drug discovery process.

Keywords

Peptide; HRMS; metabolism; bioavailability; subcutaneous; in vitro

Keywords

Peptide, high-resolution mass spectrometry, metabolism, bioavailability, subcutaneous, in vitro

1. Introduction

The development of a peptidic drug is associated with many challenges, including the optimization of absorption, distribution, metabolism, and excretion (ADME) properties [1–4]. To this purpose, there is a need for suitable *in vitro* preclinical models to study and predict their overall ADME behavior, which can significantly differ from small molecules and often require specially developed analytical tools [1,3,5–8].

Despite the many efforts being pursued in the pharmaceutical industry, no effective oral delivery of peptide therapeutics has been achieved so far [9–11], and currently the subcutaneous (SC) administration remains the most common route for this class of compounds [12–14]. After SC administration, peptides with molecular weight <10 kDa access systemic circulation directly through blood capillaries, whereas bigger proteins (molecular weight >15 kDa) tend to be absorbed mainly via the lymphatic system [15,16].

Unlike for small molecules, liver is not generally the main site of metabolism for peptide therapeutics, with a few possible exceptions [17,18]. In a typical drug discovery screening funnel, peptides which are stable in the *in vitro* plasma metabolic stability assay are prioritized for *in vivo* pharmacokinetics (PK) studies [2]. However, several works have highlighted that the SC tissue can be another important site of catabolism for peptide therapeutics of various sizes [19–24]. Since protease distribution and abundances may be significantly different for plasma and SC tissue, peptides could also undergo significant site-specific metabolism at the SC tissue. This degradation can affect the PK of a peptide, particularly bioavailability [20,24].

In previous works, peptides were incubated with tissue homogenate from human donors and/or different preclinical species to investigate peptide catabolism after SC administration, using a number of detection techniques including gamma counting [20], liquid chromatography coupled to UV detection [19,21], SDS-PAGE [22], immunoassays [23] or liquid chromatography-mass spectrometry (LC-MS) [24]. However, to the best of our knowledge, there is no description in the literature of a LC-MS *in vitro* assay used as a screening tool to evaluate metabolism at the SC injection site as the one presented in this manuscript.

The -LC-MS-based *in vitro* assay for the evaluation of the metabolism at the SC injection site (SCiMetPep assay) described in this work was developed to allow the simultaneous determination of peptide stability (half-life) and identification of proteolysis products at the injection site. The SciMetPep assay was conceived to provide a means to improve metabolic stability and to select better candidates for *in vivo* studies at a very early stage in the drug discovery process. This approach uses liquid chromatography coupled to high-resolution Orbitrap™ mass spectrometry (LC-HRMS). This last technique has become one of the most used ones for *in vitro* and *in vivo* ADME studies of small molecules and peptides due to its high selectivity and flexibility combined with a good sensitivity [25]. When full scan mode is used, LC-HRMS

enables both targeted and untargeted (qual/quan) analysis, thus allowing to monitor both the degradation profile of the parent peptides over time and the appearance of biotransformation products.

The assay was initially set up by using human insulin (HI) as a model peptide [20] and Sprague Dawley (SD) rat SC tissue supernatant (SCts). Rats are the most commonly used rodent preclinical species for peptide drug discovery [1,26,27]. Subsequently, a series of known glucagon-like peptide 1 (GLP-1) analogues were incubated with SD rat, Göttingen minipig [28,29] and human SCts. For each peptide, both the rate of parent disappearance (half-life) and the formation of metabolites were monitored. Moreover, SCiMetPep assay was applied to a series of 28 structurally related peptides to evaluate the correlation between *in vitro* metabolic stability and the SC bioavailability.

2. Materials and Methods

2.1 Chemicals and reagents

All reagents used in the SCiMetPep assay were of analytical or LC–MS grade. Water (H_2O), acetonitrile (ACN), methanol (MeOH) and formic acid (HCOOH) were purchased from Merck KGaA (Darmstadt, Germany). HI was purchased from Merck KGaA. All the other peptides used in the study were synthesized in-house. The synthesis was performed by standard solid-phase synthesis using Fmoc/t-Bu chemistry. The sequences of exenatide, lixisenatide and CP-11 and the 28 peptides of the drug discovery program were assembled on a Fmoc-Rink polystyrene resin as C-terminal amides. Liraglutide and semaglutide were synthesized on a 2-chlorotrityl chloride resin as C-terminal acid. The synthesis was performed either on a Liberty Blue peptide synthesizer (CEM Corp., Matthews NC, USA) using equimolar amounts of *N,N'*-Diisopropylcarbodiimide and oxyma [(Ethyl 2-cyano-2-(hydroximino)acetate] as activators or a Symphony peptide synthesizer (Protein Technologies Inc., Tucson AZ, USA) using equimolar amounts of HATU (O-(7-azabenzotriazol-1-yl)-N,N,N',N'-tetramethyluronium hexafluorophosphate) and a 2-fold molar excess of DIEA (N,N-diisopropylethylamine). For the synthesis of all fatty acid derivatized peptides such as, liraglutide, semaglutide and the 28 peptides of the drug discovery program, the position for lipid derivatization was incorporated as Lys(Dde) where Dde is [1-(4,4-dimethyl-2,6-dioxocyclohex-1-ylidene)ethyl]. At the end of the backbone assembly the Lys(Dde) was deprotected by treatment of 2% hydrazine in DMF and then derivatized with different linkers and fatty acids. At the end of the synthesis the peptide resins were dried and cleaved with a solution of trifluoroacetic acid (TFA)/phenol/H_2O/triisopropylsilane (87.5%/5%/5%/2.5%/ 25 ml) for 1-3 h. After cleavage from resin, all peptides were purified by reversed-phase high-pressure liquid chromatography and characterized by LC-MS.

2.1 SC tissue homogenate

SC tissue from SD rats, purchased from Charles River Laboratories Italia (Calco, Italy), was obtained *ex-vivo* from the back area of the animals. From each rat, an average of 6-7 slices (about 300 mg per slice) were

collected and used for approximately 20-25 incubations. SC tissue was stored at -80 °C in CK14 Precellys tubes (Bertin Corp., Rockville MD, USA) until analysis. Just before the analysis, the subcutaneous tissue was mixed with ice-cold PBS buffer (pH= 7.4) at a tissue/PBS (w/v) ratio of 1/4 and homogenized in a Precellys 24 Homogenizer (Bertin Corp.) at 5 000 rpm for 10 seconds. The lysate was centrifuged at 9 000 rcf at 4 °C for 30 min. The supernatant was collected and, after measuring the protein concentration via Bradford assay, it was diluted with PBS to the desired protein concentration and used for the incubation experiments. A pool of supernatant from at least three different rats was used. Male Göttingen minipig and human (male, Caucasian) SC tissues were purchased from Bioreclamation-IVT (Westbury NY, USA) and homogenized in the same conditions described for rat.

2.3 Assay validation

Freeze/thaw stability (1 cycle) and storage conditions were tested to evaluate the possibility of storing *ex-vivo* samples after collection. Four slices of SC tissue were collected from two different SD rats: one was kept in an ice bath at non-freezing temperature, while the other three were flash frozen with liquid nitrogen. The ice bath aliquot and one of the flash frozen samples were immediately used for incubation with HI (10 µM, SC proteins concentration 2 mg/mL), while the remaining flash frozen samples were kept at -80 °C and analysed after 1 and 3 months.

The reproducibility of the assay was measured using tissues from four different animals analyzed in three different days, in the same conditions described for the stability tests.

2.4 *In vitro* SCts incubation conditions

SCts was temperature-equilibrated at 37 °C for 5 min in a thermostatic shaker (500 rpm). Test compounds were added to low-bind 96-well plates using a Tecan D300e digital dispenser (Männedorf Switzerland). Stock solutions were prepared in DMSO or DMSO: H_2O mixtures to maintain DMSO concentration ≤ 0.5%. Each experiment was performed in duplicate. A control blank sample was also prepared by mixing SCts and stock solution solvent, without adding any test compounds. At each time point (0, 0.5, 1, 2, 4 h), 50 µL of SCts were collected from the incubation mixture and added to 150 µL of 1% HCOOH in ACN or MeOH, containing the IS CP-11 at a concentration of 200 ng/mL. Samples were then vortexed and centrifuged (5 min, 4500 rcf, 4 °C). The supernatant (120 µL) was transferred into a clean low-bind 96-well plate, diluted with 240 µL of 0.1% HCOOH in H_2O, and analyzed by LC-HRMS.

2.5 *In vitro* plasma incubation conditions

Human plasma incubation of four GLP-1 analogs was performed adapting a protocol from previous work [30]. Lithium-heparin plasma (purchased from Bioreclamation-IVT) was temperature-equilibrated at 37°C for 5 min in a thermostatic shaker (500 rpm). Test compounds were incubated for 4 hours at 10 µM. Each experiment was performed in duplicate. A 50 µL plasma aliquot was withdrawn at each time-point (0 and 4

h) and added to 200 µL of 1% HCOOH in MeOH containing the IS CP-11 at a concentration of 200 ng/mL. Samples were then vortexed and centrifuged (15 min, 14 000 rcf, 4 °C). The supernatant (100 µL) was transferred into a clean Lo-bind 96 deep-well plate, diluted with 100 µL 0.1% HCOOH in H_2O and analyzed by LC-HRMS. A control blank (non-spiked plasma, precipitating solution containing IS) was also prepared as a negative control.

2.6 Liquid chromatography

A Dionex Ultimate 3000 RS pump coupled to a Dionex Ultimate 3000 RS autosampler, both from Thermo Scientific (Bremen, Germany), were used for all the experiments. For the chromatographic separation, two columns were used, depending on the peptide: XSelect CSH C18 XP column (130 Å, 2.5 µm, 2.1 mm X 50 mm) and Acquity UPLC Peptide CSH C18 Column, 130 Å, 1.7 µm, 2.1 mm X 50 mm, all from Waters. Mobile phase A consisted of 0.1% HCOOH in H_2O, while mobile phase B consisted of 0.1% HCOOH in ACN. The elution gradient used for all experiments started at 0.5% mobile phase B for 0.5 min. Then, it was linearly increased to 80% mobile phase B in 4.5 min, kept constant for 1 min and taken back to the initial conditions in 0.1 min. The gradient was followed by an equilibration period of 0.9 min before the next injection (total run time 7 min). A constant flow rate of 400 µL/min was maintained. Column temperature was kept at 60 °C. A volume of 2 µL was injected.

2.7 High-resolution mass spectrometry

All analyses were conducted on an Orbitrap™ Q-Exactive mass spectrometer (Thermo Scientific) operating in ESI positive full scan/data-dependent MS/MS (FS-ddMS/MS). Each cycle contained 3 scan events: a FS (*m/z* range 200-1,600 at resolution 35,000 FWHM at 200 *m/z*) followed by 2 MS/MS fragmentation scans (resolution 17,500 FWHM at 200 *m/z*) over the 2 most abundant ions (top n= 2) of the full scan spectrum. Automatic gain control (AGC) and maximum injection time were set to 1e6 and 128 ms for FS, respectively, and 1e5 and 64 ms for dd-MS/MS, respectively. Stepped normalized collision energy (NCE), consisting of three different NCE values used within the same MS/MS event, was used for peptide fragmentation and optimized for each tested compound prior to sample analysis. The sheath and auxiliary gas (N_2) flow rate was set at 50 and 5 (arbitrary units), respectively. The temperature of the capillary was 320 °C. The S-lens RF level and the spray voltage were set to 50 (arbitrary units) and 3.2 kV, respectively.

The mass accuracy extraction window in FS mode was set at 5 ppm. For ddMS/MS analysis, an exclusion list was used: to this purpose, a control blank sample was always injected before each study and the 500 most intense *m/z* values from the blank sample were added to the exclusion list. The performance of the Orbitrap™ instrument in positive ionization mode was evaluated daily and, when required, external calibration was carried out with Exactive Calibration Kit solutions (Sigma-Aldrich and ABCR GmbH & Co. KG, Karlsruhe, Germany).

2.8 Data analysis

The peptides included in this study together with their sequences, molecular weight and LC-HRMS parameters are listed in **Table 1**. The percent of compound remaining was calculated by comparing the area ratio between the parent peptide peak area and the IS peak area at each time point to the corresponding area ratio at the zero time point. Half-life ($t_{1/2}$) was extrapolated using the expression $t_{1/2}=0.693/b$, where *b* is the slope determined in the linear fit of the natural logarithm of the percentage remaining of the parent compound versus incubation time. Detection and structure elucidation of the peptide biotransformation products formed in the SCts and human plasma incubations was carried out by using Biopharma Finder™ 2.0 (Thermo Scientific). Only metabolites with an abundance higher than 0.1% (calculated as maximum metabolite peak area*100/maximum parent peak area) were reported.

3. Results

3.1 Method Development - SC tissue supernatant preparation

The method development focused mainly on the optimization of homogenization conditions, peptide incubation and sample processing, whereas LC-HRMS conditions and the workflow for metabolite identification were mainly adapted from previous work [30].

The initial method set up was performed using prevalently SD rat SC tissue and HI as model peptide. Rat SC tissue was taken and frozen in liquid nitrogen immediately after collection. Before homogenate preparation, the tissue was kept in ice bath at room temperature for 30 min.

The SC tissue/PBS (w/v) ratio, homogenization and compound incubation conditions were the critical parameters to be optimized for a reliable and reproducible assay. For assay setup we also took into consideration homogenization protocols used in previous works [19–23]. SC tissue/PBS (w/v) ratios of 1/3, 1/4, 1/5, 1/9 were tested and 1/4 was preferred, because it provided an optimal concentration of proteins (> 1 mg/mL). Higher ratios provided extremely diluted supernatants, whereas lower ratios were not sufficient to obtain clear and reproducible extracts. The incubation was performed using the supernatant obtained after SC tissue homogenization and centrifugation. The use of the whole homogenate did not provide reproducible results. The homogenization was performed in a Precellys homogenizer at room temperature at 5 000 rpm for 10 sec. Afterwards, the whole SC homogenate was subjected to centrifugation at different speed, time and temperature conditions to separate the soluble fraction: 1) 1 000 rcf for 20 min at 4 °C, 2) 9 000 rcf for 20 min at 4 °C, 3) and 16 000 rcf for 60 min at 4 °C.

At low centrifugation speed (1 000 rcf, 20 min, 4 °C), the separation of the pellet from the supernatant was often incomplete, leading to low reproducibility and inconsistent data. In this case, the measured protein concentration in the supernatant varied significantly among different preparations, therefore this condition

was discarded. However, complete pellet separation and more reproducible SC protein concentration were observed after centrifugation at 9,000 or 16,000 rcf (see **Table 2**). Finally, 9,000 rcf for 20 min at 4 °C were selected as the optimal centrifugation conditions (See **Figure S1**).

3.2 Method Development - Incubation with test compound

HI was incubated for up to 4 h at a concentration of 1, 10 and 50 µM with SCts containing 1, 2 or 4 mg/mL of SC proteins. As shown in **Figure 1**, HI degradation in SCts followed the Michaelis-Menten kinetics. At 1 and 10 µM peptide concentrations, enzymatic degradation of insulin proceeded below Vmax and the profiles showed clear proportionality between the rate of parent disappearance and the SCts protein concentration (first-order kinetics). A protein concentration higher than 2 mg/mL was generally more difficult to obtain, therefore it was not considered for this purpose. On the basis of these results, the optimal concentrations selected for the assay were 10 µM for the test compound and 1 or 2 mg/mL for the SCts proteins. In any case, it is advisable to fine-tune peptide and protein concentration for each series. At 50 µM, proteolytic enzymes were saturated, and the degradation proceeded at Vmax (zero-order kinetics). In these conditions (high peptide concentration), it was not possible to determine the kinetics of peptide degradation and metabolite formation, but the detection and characterization of the degradation products was facilitated due to their high abundance.

3.3 Method Development - Determination of peptide degradation products

Since LC-HRMS analysis enables both targeted and untargeted analysis, it allows to monitor simultaneously the degradation profile of the parent peptide over time and the formation of the degradation products. Three metabolites were detected after incubation of HI in rat SCts all deriving from proteolytic cleavage of the parent peptide: DesB30 HI, DesB1 HI and DesB1+B30 HI (see representative extracted ion chromatograms in **Figure 2 (left)**). These metabolites were detected at both 10 and 50 µM incubation concentrations, while they were undetectable when the concentration of HI was 1 µM. Also, their relative abundance usually increased, as expected, with increasing protein concentration (**Figure 2 (right)**). The % relative abundance of the three metabolites at 50 µM resulted higher, probably due to the fact that at 10 µM (higher SCts protein/peptide ratio) the metabolites are further degraded to smaller (undetected) peptides. The observed cleavage sites were also detected after incubation with Göttingen minipig and human SCts (data not shown) and were in good agreement with those described in literature for HI after SC administration [31,32].

3.4 SCts freeze/thaw stability and stability of SC tissue upon storage at -80 °C

Different slices of SC tissue were excised from two rats. One slice was immediately homogenized while the remaining slices were frozen at -80 °C. A fresh SCts (tissue/buffer 1/4 (w/v), centrifuged at 9,000 rcf for 20 min at 4 °C) was prepared and its activity (as % HI remaining after a 4 h incubation period) before and after one freeze/thaw cycle (-20 °C) was determined. After one freeze/thaw cycle, the SCts maintained its

proteolytic activity (%CV = 8.5, n=2). The SCts activity of tissue slices after 3 months of storage at -80 °C was also determined.

The SC tissue was stable for up to 3 months when stored at -80 °C (%CV ≤ 8.7, n = 2). Therefore, it is not necessary to use freshly excised *ex-vivo* SC tissue to perform the SCiMetPep assay. This is especially important for SC tissue from species such as minipig and human that are necessarily delivered frozen to the different laboratories.

3.5 Assay reproducibility

The reproducibility of the assay was measured by incubating HI at 10 µM in rat SCts (tissue/buffer 1/4 (w/v), centrifuged at 9,000 rcf for 20 min at 4 °C) from four animals, on three different days (SC proteins concentration 2 mg/mL) and comparing the half-life values. Incubation using SC tissue taken from different rats gave reproducible results, with intra-day and inter-day %CV being ≤ 24.4% (n = 4) and 20.9%, (n = 4), respectively (**Figure 3**).

3.6 Analysis of GLP-1 analogues

A series of known peptides were incubated with SCts from rat, minipig and human at the conditions optimized with HI to further evaluate the assay. Since SCts protein concentration in human and minipig SC tissue was generally lower (1-2 mg/mL) than rat (3-4 mg/mL) after centrifugation, it was decided to perform incubations at 1 mg/mL SCts protein concentration when testing all three species together.

The investigated peptides included human GLP-1 analogues exenatide, lixisenatide, liraglutide and semaglutide. As it is well known, human GLP-1 is highly metabolized mainly by two proteases: dipeptidyl peptidase IV (DPP-IV) and neutral endopeptidase (NEP), making it impossible to use it as a drug [33]. Exenatide and lixisenatide, which have approximately 50% sequence homology with GLP-1, are resistant to DPP-IV and are poor substrates for NEP. Since they survive longer in the circulation, they can be administered to humans twice- and once-daily respectively [17,33]. Both compounds have *in vitro* half-life of approximately 4 and 9 hours in rat and in human plasma, respectively [34–36]. Liraglutide and semaglutide have respectively 97% and 94% sequence homology with GLP-1 and a fatty acid (liraglutide) or diacid (semaglutide) side chain. These lipid moieties act as PK enhancers by increasing protein binding, and protect the two peptides from proteolytic degradation in plasma [17,35,37,38]. High *in vitro* stability of these four compounds was confirmed also in our experiments using human plasma (**see Figure S2**).

The results of the incubation of the four peptides in the SCts from rat, minipig and human are summarized in **Figure 4**. Lixisenatide was completely degraded having $t_{1/2}$ < 0.5 hours in all species. The other three peptides showed higher stability. In particular, liraglutide and exenatide turned out to be the most stable in all three species, with $t_{1/2}$ higher than 4 hours, followed by semaglutide.

The cleavage sites for the four peptides are shown in **Figure 5**, whereas **Tables S1-S4** contain the complete list of metabolites. Numerous cleavage sites were identified. The cleavage at position 8-9 (typical for DPP-IV) was observed only for liraglutide, but not for exenatide, lixisenatide (in which a Gly residue was present at position 8 instead of Ala) and semaglutide (in which Ala_8 was substituted by the non-natural amino acid aminoisobutiryc acid (Aib)). Each peptide showed also one or more NEP-related proteolytic cleavages (positions 15-16, 18-19, 19-20, 27-28, 28-29, and 31-32).

The most important cleavage sites for liraglutide and semaglutide were observed at the Ser_{18}-Tyr_{19} and Tyr_{19}-Leu_{20} amide bonds in all three species. The products from Tyr_{19}-Leu_{20} cleavage were also observed as major *in vivo* metabolites in human for both liraglutide and semaglutide after SC administration [17,39]. No metabolites were detected after *in vitro* incubation of the two peptides with human plasma. This result may suggest that these metabolites are formed in the SC tissue (although their formation in other organs/compartments cannot be fully excluded).

The Phe_{12}-Thr_{13}, Ser_{17}-Lys_{18}, Arg_{26}-Leu_{27}, Leu_{27}-Phe_{28} and Phe_{28}-Ile_{29} bonds were susceptible to degradation in both exenatide and lixisenatide, particularly in SD rat and human. The products of Arg_{26}-Leu_{27} and Phe_{28}-Ile_{29} were also previously detected *in vivo* (SD rats) after SC administration by Copley et al. [40]. Additionally, lixisenatide showed extensive degradation at the lysine-rich C-terminus in all species. Following *in vitro* incubation with human plasma, only one exenatide metabolite (Glu_9-Ser_{45}) and two lixisenatide metabolites (Glu_9-Ser_{44} and His_7-Lys_{50}) were detected, with a low relative abundance (data not shown).

On the whole, we found a good correlation between the proteolytic products identified in SCts incubations and the degradation products circulating in plasma after SC administration described in the literature, but also between *in vitro* metabolic stability and *in vivo* SC bioavailability [38,41–46].

3.7 Correlation between *in vitro* metabolic stability and *in vivo* SC bioavailability

The effect of metabolism at the SC injection site on peptide bioavailability has been described in several works [20,24,47]. In order to evaluate the correlation between *in vitro* metabolic stability and *in vivo* SC bioavailability, 28 structurally related peptides from a drug discovery program were analyzed with the SCiMetPep assay. These peptides with a molecular weight in the range of 3-5 kDa and numerous sequence modifications and fatty acids as PK enhancer moieties, showed a good variety of bioavailability, from very low to very high, after SC administration in rats. Therefore, they were chosen as an optimal testing set for our assay. **Figure 6** shows a representative example observed in this series: when the parent peptide was administered SC to 3 SD rats, the data obtained from rat I and II were significantly different from those obtained from rat III. In particular, rat III showed twice the bioavailability of rats I and II. The metabolite ID analysis of the samples revealed that the bioavailability difference was due to the formation of a major metabolite (M8) in rats I and II, which was generated in smaller amounts in rat III. Moreover, M8 was

present as a major metabolite only after SC administration, whereas it was less abundant after IV administration, clearly indicating that this metabolite was generated at the injection site. Results from SD rat SCts incubation are shown in **Figure 7**. A reasonably good correlation (R^2= 0.53) was observed between the *in vivo* SC bioavailability and the *in vitro* stability (expressed as percent remaining at 4 h).

4. Discussion

Plasma and SC tissue are potentially two major sites of metabolism for peptidic drugs after SC administration. Differently from small molecules, that penetrate cells and are usually metabolized in the liver or other organs by cytochrome P450 or phase II enzymes, peptides are generally confined in the plasma compartment and subject to proteolytic metabolism from proteases [1,4].

Peptides with low protein binding, such as HI, are likely to be exposed to proteases not only located at the injection site, but also in plasma, and are generally subject to urinary excretion [40,48]. For these peptides, the proteolytic metabolism can occur in both sites, and it is mainly dependent of the distribution of the proteases and their affinity for the peptide. Substrate specificity and tissue distribution of proteases has not yet been fully characterized but a good amount of data can be found in the literature or in several online databases [8,49–51]. On the other hand, peptides with high protein binding, such as lipidated peptides, are more protected from both plasma proteases and glomerular filtration [52]. In this case, catabolism at the SC injection site could be particularly important, due to a lower protein concentration. Albumin concentration in the interstitial fluid of the human SC tissue is approximately one-seventh of the albumin concentration in plasma, as measured by Ellmerer *et al.* [53]. In these conditions, the unbound fraction of the peptide could be significantly higher than in plasma, making the compound more susceptible to metabolism. The SCiMetPep assay can be useful for both low- and high-affinity protein binding peptides to identify metabolic cleavages that are specific for the SC tissue and not occurring in plasma. This further *in vitro* characterization can be used before *in vivo* studies to prioritize compounds with good stability and to eliminate potential metabolic liabilities as early as possible.

In a drug discovery program, it is important to know whether the degradation in the subcutaneous tissue is affecting the peptide absorption [54]. Results from the analysis of the 28 peptides from a drug discovery program showed that when *in vivo* metabolism at the injection site is prevalent (**Figure 6**), there is a reasonably good *in vitro/in vivo* correlation (**Figure 7**). Therefore, the SciMetPep assay can also provide some indication whether the compound will have a low or high *in vivo* bioavailability, but supposedly only when the metabolic stability in the SC tissue is the main parameter driving absorption. Future studies will focus on evaluating different peptide series to better characterize this relationship.

The effect of the metabolism at the injection site on bioavailability can be evident in some cases, for example when comparing lixisenatide and exenatide (**Figure 4**). These two peptides differ only for the

addition of six lysine residues in lixisenatide and the deletion of a proline. While both peptides are stable in plasma, lixisenatide was degraded much faster than exenatide in the SCiMetPep assay, particularly at the lysinated C-terminus. This latter site-specific degradation is most probably the cause of the low SC bioavailability reported in the literature for this peptide (3% in rat, 32% in human) compared to exenatide (62% in rat, 66% in minipig, 97% in human).

However, the SC absorption is clearly a multifactorial process, and therefore metabolic degradation is not the only parameter potentially affecting bioavailability after SC administration. Besides absorption and metabolism in the lymphatic system, which is less important for peptides and small proteins, another phenomenon that can play an important role is peptide aggregation. In fact, at high concentrations at the injection site, peptides can form oligomeric aggregates, especially if lipidated due to their amphiphilic nature. Oligomerization can significantly modify the pharmacokinetic behavior (absorption and clearance) of a peptide [52,55]. For example, liraglutide has a strong tendency to form oligomeric aggregates at the injection site, which is also responsible for its prolonged release into the circulation [43]. Wang et al. hypothesized that the formation of micelle-like oligomers at high peptide concentrations, such as in the SC site, could provide good metabolic stability [52]. This could explain the extremely high stability of liraglutide in our assay, even higher than semaglutide which has a stronger albumin binding affinity and resistance to DPP-IV [38] but a much lower tendency to form aggregates (IRBM Science Park, unpublished data). In any case, a deep investigation on the influence of peptide aggregation on SC bioavailability and metabolism was out of the scope of this work.

5. Conclusions

In this manuscript we described the development of the SCiMetPep assay, an efficient and reproducible LC-HRMS *in vitro* assay to assess peptide metabolism in the SC tissue. The integrated workflow allows to obtain both the degradation rate of the parent peptides and the identification of its metabolites.

The procedures for tissue homogenization, incubation conditions, sample preparation and LC-HRMS analysis were evaluated, optimized and validated using HI as a model peptide. Then the method was applied to a series of known GLP-1 analogs and the identified cleavage sites were in good agreement with those detected in vivo after SC administration that are described in literature. Finally, a fairly good correlation was found in a series of peptides from a drug discovery program between *in vitro* SC metabolic stability and *in vivo* SC bioavailability.

The data presented in this manuscript support the use of the SCiMetPep assay as a powerful tool for prioritization of peptides with lower potential to be degraded in the subcutaneous tissue, avoiding unnecessary *in vivo* experiments with benefits in terms of 3Rs (replacement, reduction, refinement) improvement, time and money saving. Moreover, this assay can simultaneously provide information on the

metabolic soft spots observed in the subcutaneous space than can be different from plasma and hence guide medicinal chemists in the synthesis of new analogs.

6. Acknowledgements

Dr. Stephane Illiano and Dr. Sergio Mallart from Sanofi-Aventis (Chilly Mazarin, France) are gratefully acknowledged for the fruitful discussion and for providing some of the peptides used in this study. The authors would also like to thank the following persons from IRBM Science Park: Fabio Bonelli, Maria Veneziano, Fulvia Caretti, Fabrizio Colaceci, Romina Sasso and Cristiano Terzo for technical support and useful suggestions, and Alessia Santoprete, Federica Orvieto, Paola Magotti, Sonia Del Rizzo, Daniela Roversi, Roberto Iaccarino, Federica Tucci and Federica Rulli for the synthesis of the peptides.

7. Compliance with Ethical Standards

All authors are currently employed at IRBM Science Park and declare no conflicts of interest. All institutional and national guidelines for the care and use of laboratory animals were followed.

8. References

[1] T. Katsila, A.P. Siskos, C. Tamvakopoulos, Peptide and protein drugs: the study of their metabolism and catabolism by mass spectrometry, Mass Spectrom. Rev. 31 (2012) 110–133.

[2] L. Di, Strategic approaches to optimizing peptide ADME properties, AAPS J. 17 (2015) 134–143.

[3] J.H. Lin, Pharmacokinetics of biotech drugs: peptides, proteins and monoclonal antibodies, Curr. Drug Metab. 10 (2009) 661–691.

[4] P. Timmerman, B. Lausecker, B. Barosso, P. van Amsterdam, S. Luedtke, J. Dijksman, “Large Meets Small”: connecting the bioanalytical community around peptide and protein bioanalysis with LC-MS(/MS), Bioanalysis. 4 (2012) 627–631.

[5] R.N.X. Xu, L.M. Fan, M.J. Rieser, T.A. El-Shourbagy, Recent advances in high-throughput quantitative bioanalysis by LC-MS/MS, J. Pharm. Biomed. Anal. 44 (2007) 342–355.

[6] M. Ewles, L. Goodwin, Bioanalytical approaches to analyzing peptides and proteins by LC--MS/MS, Bioanalysis. 3 (2011) 1379–1397.

[7] T. Prueksaritanont, C. Tang, ADME of biologics-what have we learned from small molecules?, AAPS J. 14 (2012) 410–419.

[8] T. Radchenko, A. Brink, Y. Siegrist, C. Kochansky, A. Bateman, F. Fontaine, et al., Software-aided approach to investigate peptide structure and metabolic susceptibility of amide bonds in peptide drugs based on high resolution mass spectrometry, PLoS One. 12 (2017) e0186461.

[9] D.J. Craik, D.P. Fairlie, S. Liras, D. Price, The future of peptide-based drugs, Chem. Biol. Drug Des. 81 (2013) 136–147.

[10] J. Renukuntla, A.D. Vadlapudi, A. Patel, S.H.S. Boddu, A.K. Mitra, Approaches for enhancing oral bioavailability of peptides and proteins, Int. J. Pharm. 447 (2013) 75–93.

[11] A. Muheem, F. Shakeel, M.A. Jahangir, M. Anwar, N. Mallick, G.K. Jain, et al., A review on the strategies for oral delivery of proteins and peptides and their clinical perspectives, Saudi Pharm. J. 24 (2016) 413–428.

[12] T.A. McDonald, M.L. Zepeda, M.J. Tomlinson, W.H. Bee, I.A. Ivens, Subcutaneous administration of biotherapeutics: current experience in animal models, Curr. Opin. Mol. Ther. 12 (2010) 461–470.

[13] A.L. Lewis, J. Richard, Challenges in the delivery of peptide drugs: an industry perspective, Ther. Deliv. 6 (2015) 149–163.

[14] B.J. Bruno, G.D. Miller, C.S. Lim, Basics and recent advances in peptide and protein drug delivery, Ther. Deliv. 4 (2013) 1443–1467.

[15] A. Supersaxo, W.R. Hein, H. Steffen, Effect of molecular weight on the lymphatic absorption of water-soluble compounds following subcutaneous administration, Pharm. Res. 7 (1990) 167–169.

[16] D.N. McLennan, C.J.H. Porter, S.A. Charman, Subcutaneous drug delivery and the role of the lymphatics, Drug Discov. Today Technol. 2 (2005) 89–96.

[17] L. Jensen, H. Helleberg, A. Roffel, J.J. van Lier, I. Bjørnsdottir, P.J. Pedersen, E. Rowe, J. Derving Karsbøl, M.L. Pedersen, Absorption, metabolism and excretion of the GLP-1 analogue semaglutide in humans and nonclinical species, Eur. J. Pharm. Sci. 104 (2017) 31–41.

[18] P.B. Watkins, The role of cytochromes P-450 in cyclosporine metabolism. J. Am. Acad. Dermatol. 23 (1990) 1301–1309.

[19] H.W. Ryou, J.W. Lee, K. a Yoon, E.S. Park, S.C. Chi, Effect of protease inhibitors on degradation of recombinant human epidermal growth factor in skin tissue, Arch. Pharm. Res. 20 (1997) 34–38.

[20] M. Takeyama, T. Ishida, N. Kokubu, F. Komada, S. Iwakawa, K. Okumura, R. Hori, Enhanced bioavailability of subcutaneously injected insulin by pretreatment with ointment ccontaining protease inhibitors, Pharm. Res. An Off. J. Am. Assoc. Pharm. Sci. 8 (1991) 60–64.

[21] M. Bi, J. Singh, Degradation of luteinizing hormone releasing hormone in buccal, liver, nasal and skin tissues, Int. J. Pharm. 175 (1998) 269–273.

[22] W. Wang, N. Chen, X. Shen, P. Cunningham, S. Fauty, K. Michel, B. Wang, X. Hong, C. Adreani, C.N. Nunes, C.V. Johnson, K.C. Yin, M. Groff, Y. Zou, L. Liu, L. Hamuro, T. Prueksaritanont, Lymphatic transport and catabolism of therapeutic proteins after subcutaneous administration to rats and dogs, Drug Metab. Dispos. 40 (2012) 952–962.

[23] A. Fatouros, Y. Lidén, B. Sjöström, Recombinant factor VIII SQ--stability of VIII: C in homogenates from porcine, monkey and human subcutaneous tissue, J. Pharm. Pharmacol. 52 (2000) 797–805.

[24] Y. Ito, H. Murano, N. Hamasaki, K. Fukushima, K. Takada, Incidence of low bioavailability of leuprolide acetate after percutaneous administration to rats by dissolving microneedles, Int. J. Pharm. 407 (2011) 126–131.

[25] L. Dillen, F. Cuyckens, High-resolution MS: first choice for peptide quantification?, Bioanalysis. 5 (2013) 1145–1148.

[26] K. Fosgerau, T. Hoffmann, Peptide therapeutics: Current status and future directions, Drug Discov. Today. 20 (2015) 122–128.

[27] W.F. Richter, S.G. Bhansali, M.E. Morris, Mechanistic determinants of biotherapeutics absorption following SC administration, AAPS J. 14 (2012) 559–570.

[28] P. Heining, T. Ruysschaert, The use of minipig in drug discovery and development, Toxicol. Pathol. 44 (2016) 467–473.

[29] V.K. Singh, K.D. Thrall, M. Hauer-Jensen, Minipigs as models in drug discovery, Expert Opin. Drug Discov. 11 (2016) 1131–1134.

[30] S. Esposito, R. Mele, R. Ingenito, E. Bianchi, F. Bonelli, E. Monteagudo, et al., An efficient liquid chromatography-high resolution mass spectrometry approach for the optimization of the metabolic stability of therapeutic peptides, Anal. Bioanal. Chem. 409 (2017) 2685–2696.

[31] M.R. Sommerfeld, G. Müller, G. Tschank, G. Seipke, P. Habermann, R. Kurrle, N. Tennagels, In vitro metabolic and mitogenic signaling of insulin glargine and its metabolites, PLoS One. 5 (2010) e9540.

[32] A. Thomas, P. Brinkkötter, W. Schänzer, M. Thevis, Metabolism of human insulin after subcutaneous administration: A possible means to uncover insulin misuse, Anal. Chim. Acta. 897 (2015) 53–61.

[33] C.F. Deacon, Therapeutic strategies based on glucagon-like peptide 1, Diabetes. 53 (2004) 2181–2189.

[34] P. and F.S.B. Evaluation and Licensing Division, L. and W. Ministry of Health, Review Report - Lyxumia Subcutaneous Injection 300 μg, 2013. https://www.pmda.go.jp/files/000153885.pdf (accessed March 19, 2018).

[35] J. Han, L. Sun, X. Huang, Z. Li, C. Zhang, H. Qian, W. Huang, Novel coumarin modified GLP-1 derivatives with enhanced plasma stability and prolonged in vivo glucose-lowering ability, Br. J. Pharmacol. 171 (2014) 5252–5264.

[36] J. Chen, L. Yu, L. Wang, X. Fang, L. Li, W. Li, Stability of synthetic exendin-4 in human plasma in vitro, Protein Pept. Lett. 14 (2007) 19–25.

[37] K. Madsen, L.B. Knudsen, H. Agersoe, P.F. Nielsen, H. Thøgersen, M. Wilken, N.L. Johansen, Structure−activity and protraction relationship of long-acting glucagon-like peptide-1 derivatives: importance of fatty acid length, polarity, and bulkiness, J. Med. Chem. 50 (2007) 6126–6132.

[38] J. Lau, P. Bloch, L. Schäffer, I. Pettersson, J. Spetzler, J. Kofoed, K. Madsen, L.B. Knudsen, J. McGuire, D.B. Steensgaard, H.M. Strauss, D.X. Gram, S.M. Knudsen, F.S. Nielsen, P. Thygesen, S. Reedtz-Runge, T. Kruse, Discovery of the once-weekly glucagon-Like Peptide-1 (GLP-1) analogue semaglutide, J. Med. Chem. 58 (2015) 7370–7380.

[39] M. Malm-Erjefalt, I. Bjornsdottir, J. Vanggaard, H. Helleberg, U. Larsen, B. Oosterhuis, J.J van Lier, M. Zdravkovic, A.K. Olsen, Metabolism and excretion of the once-daily human glucagon-like peptide-1 analog liraglutide in healthy male subjects and its in vitro degradation by dipeptidyl peptidase IV and neutral endopeptidase, Drug Metab. Dispos. 38 (2010) 1944–1953.

[40] K. Copley, K. McCowen, R. Hiles, L. Nielsen, A. Young, D. Parkes, Investigation of exenatide elimination and its in vivo and in vitro degradation, Curr. Drug Metab. 7 (2006) 367–374.

[41] D. Parkes, C. Jodka, P. Smith, S. Nayak, L. Rinehart, R. Gingerich, K. Chen, A. Young, Pharmacokinetic actions of exendin-4 in the rat: comparison with glucagon-like peptide-1, Drug Dev. Res. 53 (2001) 260–267.

[42] European Medicines Agency, Assessment Report for Byetta. http://www.ema.europa.eu/docs/en_GB/document_library/EPAR_-_Scientific_Discussion/human/000698/WC500051842.pdf, 2006 (accessed December 11, 2017).

[43] European Medicines Agency, Assessment Report for Victoza. http://www.ema.europa.eu/docs/en_GB/document_library/EPAR_-_Public_assessment_report/human/001026/WC500050016.pdf, 2009 (accessed November 3, 2017).

[44] CHMP, Assessment report for Lyxumia. http://www.ema.europa.eu/docs/en_GB/document_library/EPAR_-_Public_assessment_report/human/002445/WC500140449.pdf, 2012 (accessed November 2, 2017).

[45] Center for Drug Evaluation and Research, application number: 208471Orig1s000 (lixisenatide injection). https://www.accessdata.fda.gov/drugsatfda_docs/nda/2016/208471Orig1s000ClinPharmR.pdf, 2015 (accessed February 7, 2018).

[46] Food and Drug Administration, OZEMPIC (semaglutide) injection, for subcutaneous use. https://www.accessdata.fda.gov/drugsatfda_docs/label/2017/209637lbl.pdf, 2017 (accessed February 6, 2018).

[47] C. Adessi, C. Soto, Converting a peptide into a drug: Strategies to improve stability and bioavailability, Curr. Med. Chem. 9 (2002) 963–978.

[48] M. Serada, A. Sakurai-Tanikawa, M. Igarashi, K. Mitsugi, T. Takano, K. Shibusawa, et al., The role of the liver and kidneys in the pharmacokinetics of subcutaneously administered teriparatide acetate in rats, Xenobiotica. 42 (2012) 398–407. doi:10.3109/00498254.2011.622811.

[49] MEROPS - the Peptidase Database. httpS://www.ebi.ac.uk/merops/index.shtml (accessed November 17, 2017).

[50] The Human Protein Atlas, (2018). https://www.proteinatlas.org/ (accessed July 2, 2018).

[51] R. Kappelhoff, X.S. Puente, C.H. Wilson, A. Seth, C. López-Otín, C.M. Overall, Overview of transcriptomic analysis of all human proteases, non-proteolytic homologs and inhibitors: Organ, tissue and ovarian cancer cell line expression profiling of the human protease degradome by the CLIP-CHIP™ DNA microarray, Biochim. Biophys. Acta - Mol. Cell Res. 1864 (2017) 2210–2219.

[52] Y. Wang, A. Lomakin, S. Kanai, R. Alex, S. Belli, M. Donzelli, et al., The molecular basis for the prolonged blood circulation of lipidated incretin peptides: Peptide oligomerization or binding to serum albumin?, J. Control. Release. 241 (2016) 25–33. doi:10.1016/j.jconrel.2016.08.035.

[53] M. Ellmerer, L. Schaupp, G.A. Brunner, G. Sendlhofer, A. Wutte, P. Wach, et al., Measurement of interstitial albumin in human skeletal muscle and adipose tissue by open-flow microperfusion., Am. J. Physiol. Endocrinol. Metab. 278 (2000) E352–6. http://www.ncbi.nlm.nih.gov/pubmed/10662720 (accessed September 19, 2017).

[54] S.G. Roller, Chapter 8. ADME Properties of Peptide Therapeutics in Drug Discovery and Development, in: V. Srivastava (Ed.), Pept. Drug Discov. Challenges New Ther., The Royal Society of Chemistry, 2017: pp. 223–251. doi:10.1039/9781788011532-00223.

[55] D.K. Clodfelter, A.H. Pekar, D.M. Rebhun, K.A. Destrampe, H.A. Havel, S.R. Myers, et al., Effects of Non-Covalent Self-Association on the Subcutaneous Absorption of a Therapeutic Peptide, Pharm. Res. 15 (1998) 254–262. doi:10.1023/A:1011918719017.

Figure 1

Degradation profile of human insulin in SD rat SCts at different peptide/ SCts protein ratio.

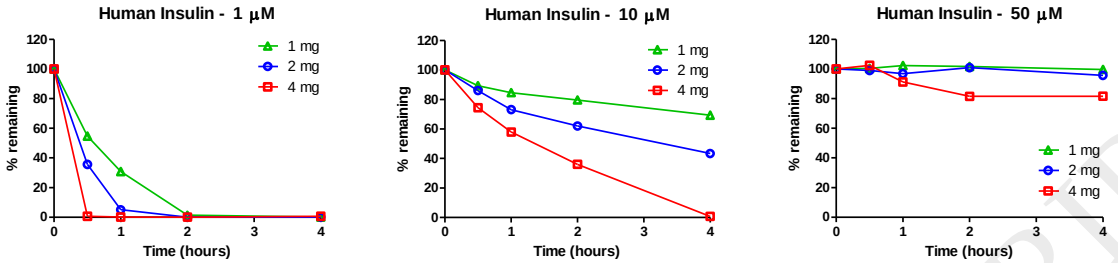

[HI] - µM	1			10			50		
[SCts protein] – mg/mL	1 mg	2 mg	4 mg	1 mg	2 mg	4 mg	1 mg	2 mg	4 mg
t1/2 (hours)	<0.5	<0.5	<0.5	> 4	3.43	0.56	> 4	> 4	> 4

Figure 2

Left: representative extracted ion chromatograms of HI and its major metabolites after 4 h incubation in SD rat SCts (HI concentration: 50 µM; SCts protein concentration: 2 mg/mL). Right: relative abundances of HI metabolites as a function of SCts protein concentration (HI concentration: 10 and 50 µM; SCts protein concentration: 1, 2 and 4 mg/mL) expressed as % parent maximum peak area. No HI metabolites were detected after 1 µM incubations regardless of the SCts protein concentration.

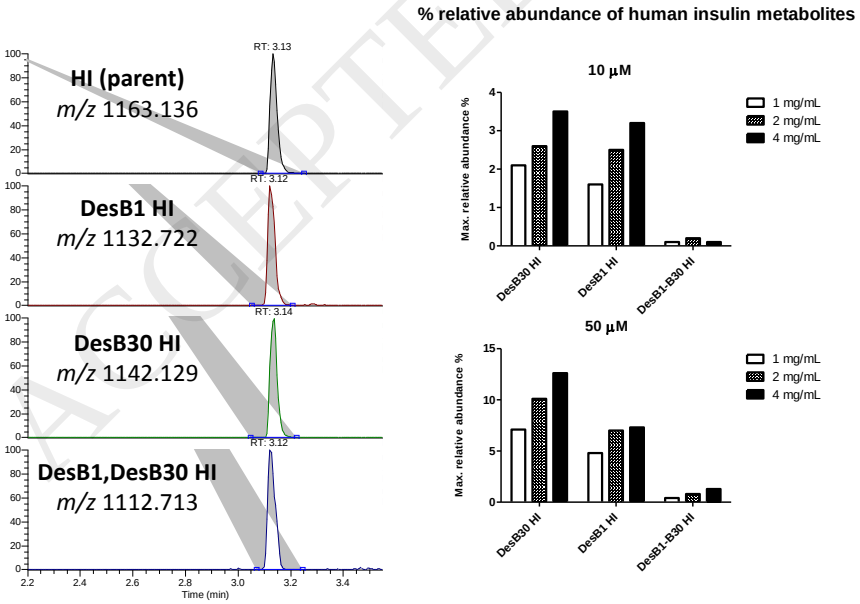

Figure 3

Intra- and inter-day reproducibility of HI incubation in SD rat SCts (HI concentration: 10 µM; SCts protein concentration: 2 mg/mL).

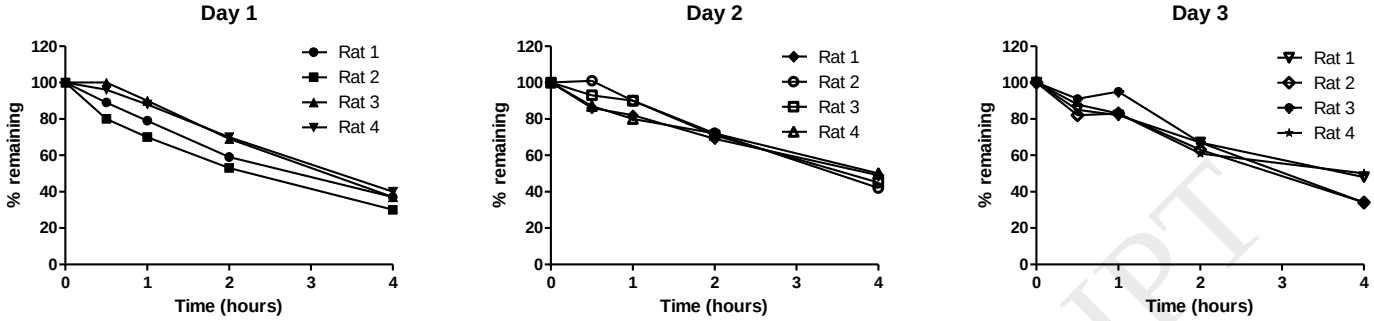

Sample ID	$t_{1/2}$ (h)
SCts rat 1	2.7
SCts rat 2	2.4
SCts rat 3	2.6
SCts rat 4	3.0
Average $t_{1/2}$ (h)	**2.7**
SD	**0.2**
%CV	**9.0**

Sample ID	$t_{1/2}$ (h)
SCts rat 1	4.0
SCts rat 2	3.0
SCts rat 3	3.4
SCts rat 4	4.2
Average $t_{1/2}$ (h)	**3.6**
SD	**0.6**
%CV	**15.5**

Sample ID	$t_{1/2}$ (h)
SCts rat 1	3.9
SCts rat 2	2.6
SCts rat 3	2.5
SCts rat 4	3.9
Average $t_{1/2}$ (h)	**3.2**
SD	**0.8**
%CV	**24.4**

Figure 4

Degradation profiles of GLP-1 analogues after incubation in human, SD rat and Göttingen minipig SCts (peptide concentration: 10 µM; SCts protein concentration: 1 mg/mL). Among these peptides, lixisenatide had the lowest bioavailability after SC administration, whereas liraglutide, exenatide and semaglutide all showed good *in vivo* SC absorption. A full list of the metabolites for each peptide is included in Table S1-S4. NA: data not available from literature.

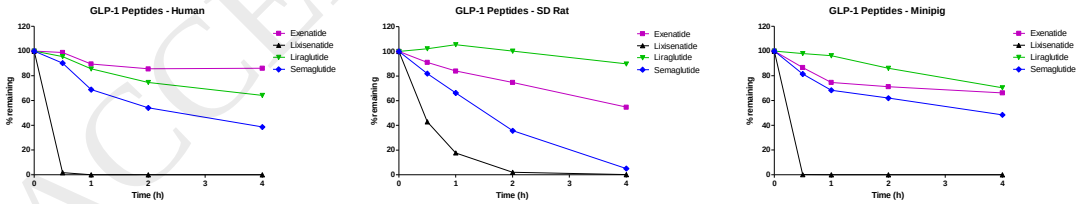

Peptide	Human			SD Rat			Minipig		
	% remaining at 4 hours	Half-life (hours)	F (%) [Reference]	% remaining at 4 hours	Half-life (hours)	F (%) [Reference]	% remaining at 4 hours	Half-life (hours)	F (%) [Reference]
Exenatide	86	> 4	97 [42]	55	> 4	62 [41]	66	> 4	NA
Lixisenatide	0	< 0.5	32 [45]	0	< 0.5	3 [44]	0	< 0.5	NA
Liraglutide	64	> 4	55 [43]	90	> 4	NA	70	> 4	66 [38]
Semaglutide	39	3.0	89 [46]	5	0.9	NA	49	> 4	94 [38]

Figure 5

Summary of the cleavage sites identified in the four GLP-1 analogues after incubation in human (black arrows), SD rat (grey) and Göttingen minipig (white) SCts. All compounds were incubated at 10 µM with 1 mg/mL protein concentration. The cleavage sites corresponding to the top 3 metabolites (in terms of MS signal response) for each species are highlighted with a red asterisk. A full list of the metabolites for each peptide is included in Table S1-S4.

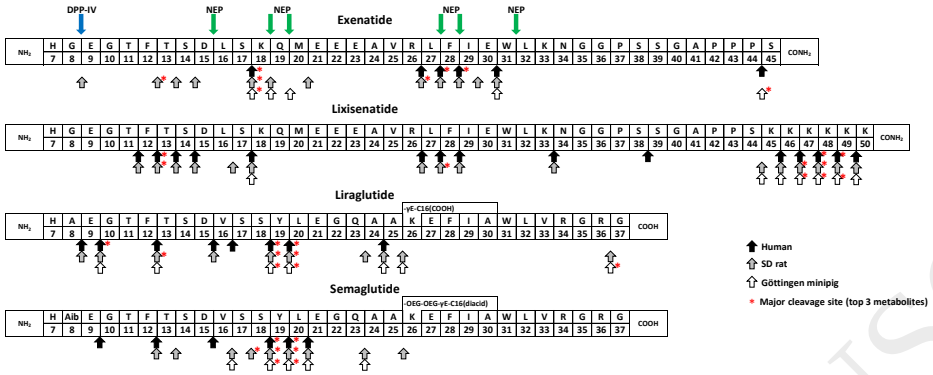

Figure 6

Influence of metabolism at the injection site on SC bioavailability of a peptide. After SC administration of the parent peptide to 3 SD rat, rat I and II showed lower bioavailability than III due to higher abundance of a major metabolite (M8) generated at the SC injection site. The abundance of M8 after IV administration was much lower. Cmax= maximum concentration; Tmax= maximum concentration time; AUC= area under curve; t½= half-life; F= bioavailability.

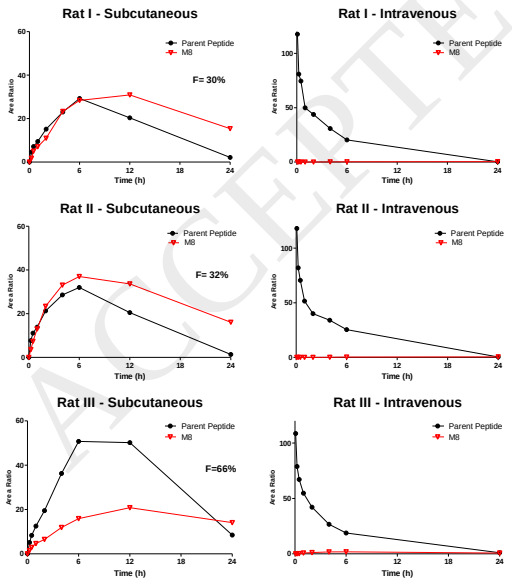

PK parameters – Subcutaneous administration							
Parameter	Cmax	Tmax	AUC	AUC Extrap	t1/2	F(0-24h)	F(0-∞)
Units	µM	Hours	µM*Hours	µM*Hours	Hours	%	%
SC – Rat I	0.62	6	8.3	8.6	4.6	29	30
SC – Rat II	0.68	6	9.0	9.2	3.8	32	32
SC – Rat III	1.07	6	17.3	19.0	6.5	61	66

Figure 7

Correlation between *in vitro* stability of peptides incubated with SD rat SCts and *in vivo* bioavailability after SC administration (peptide concentration: 10 µM; SCts protein concentration: 2 mg/mL).

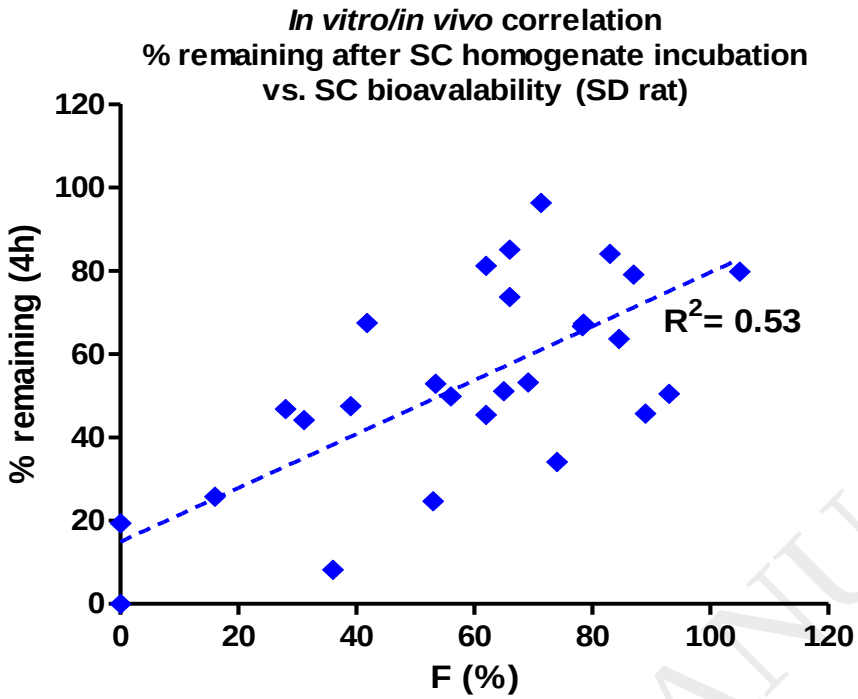

Table 1

List of known peptides included in the study.

Peptide	Sequence	Monoisotopic mass (Da)	RT min	*m/z*	Charge State
Human Insulin	GIVEQCCTSICSLYQLENYCN/FVNQHLCGSHLVEALYLVCGERGFFYTPKT (3 ss)	5803.638	3.12	1162.330	$[M+5H]^{5+}$
Exenatide	HGEGTFTSDLSKQMEEEAVRLFIEWLKNGGPSSGAPPPS-$CONH_2$	4184.027	3.15	837.813	$[M+5H]^{5+}$
Lixisenatide	HGEGTFTSDLSKQMEEEAVRLFIEWLKNGGPSSGAPPSKKKKKK-$CONH_2$	4855.544	2.63	694.657	$[M+7H]^{7+}$
Liraglutide	HAEGTFTSDVSSYLEGQAAK(γE-C16(COOH))EFIAWLVRGRG	3748.947	4.00	937.998	$[M+4H]^{4+}$
Semaglutide	H-Aib-EGTFTSDVSSYLEGQAAK(OEG-OEG-γE-C16(diacid))EFIAWLVRGRG	4111.115	3.79	1029.287	$[M+4H]^{4+}$
CP-11 (IS)	ILKKWPWWPWRRK-NH_2	1879.112	1.91	470.533	$[M+4H]^{4+}$

NOTE: 3 ss= 3 disulfide bonds: 2 inter-chain (A7-B7 and A20-B19) and one intra-chain (A6-A11); γE= gamma-glutamic acid; OEG= oligoethylene glycol

Table 2

Protein concentration after SC tissue homogenate centrifugation in different conditions (SC tissue/buffer ratio 1/4 (w/v)).

		SC Tissue Homogenate Centrifugation Conditions		
		1 000 rcf – 20 min 4 °C	9 000 rcf – 20 min 4 °C	16 000 rcf - 60 min 4 °C
	Average (n=4)	4.1	3.3	4.3

SC supernatant protein concentration (mg/mL)	SD	1.6	0.7	1.2
	%CV	38.8	22	28.6